ST.TERESA'S COLLEGE

(AUTONOMOUS)

ERNAKULAM

FINAL YEAR M.Sc. PHYSICS

PROJECT REPORT

2021-2022

TEMPERATURE CONTROLLED SYNTHESIS OF ZINC FERRITES AND ITS NANOCOMPOSITES FOR PHOTOCATALYTIC AND ANTIBACTERIAL APPLICATIONS

PROJECT REPORT

Submitted by

FATHIMA NOURIN V. A.

Register No: AM20PHY005

Under the guidance of

Ms. MINU PIUS

In partial fulfillment of the requirement for the award

Of

MASTER DEGREE OF SCIENCE IN PHYSICS

ST.TERSAS'S COLLEGE (AUTONOMOUS),

ERNAKULAM, KOCHI-682011

DEPARTMENT OF PHYSICS AND CENTRE FOR RESEARCH

ST. TERESA'S COLLEGE (AUTONOMOUS), ERNAKULAM

M.Sc. PHYSICS PROJECT REPORT

Name : FATHIMA NOURIN V A

Register Number : AM20PHY005

Year of Work : 2020-2022

This is to certify that the project "**TEMPERATURE CONTROLLED SYNTHESIS OF ZINC FERRITES AND ITS NANOCOMPOSITES FOR PHOTOCATALYTIC AND ANTIBACTERIAL APPLICATIONS**" is the work done by **Fathima Nourin V A.**

Ms.Minu Pius 10/6/2022

Staff Member in charge

Dr. Priya Parvathi Ameena Jose

Head of the Department

Submitted for the university examination held in St. Teresa's College, Ernakulam.

Examiners

1. Dr. Issac Paul
2. Dr. Gisthamol Mathew

ST.TERESA'S COLLEGE

(AUTONOMOUS)

ERNAKULAM

CERTIFICATE

This is to certify that the project report titled "**TEMPERATURE CONTROLLED SYNTHESIS OF ZINC FERRITES AND ITS NANOCOMPOSITES FOR PHOTOCATALYTIC AND ANTIBACTERIAL APPLICATIONS**" submitted by **FATHIMA NOURIN V A**, towards partial fulfillment of the requirements for the award of the degree of Masters of Physics is a record of bonafide work carried out by them during the academic year 2021-2022

Supervising guide

10/6/2022

Ms. Minu Pius

Assistant professor

Department of Physics

Head of the department

Dr. Priya Parvathi Ameena Jose

Assistant Professor

Department of Physics

PLACE: Ernakulum

DATE: 13-06-22

TEMPERATURE CONTROLLED SYNTHESIS OF ZINC FERRITES AND ITS NANOCOMPOSITES FOR PHOTOCATALYTIC AND ANTIBACTERIAL APPLICATIONS

DECLARATION

I, FATHIMA NOURIN V A, Register No.AM20PHY005, hereby declare that this project entitled **"TEMPERATURE CONTROLLED SYNTHESIS OF ZINC FERRITES AND ITS NANOCOMPOSITES FOR PHOTOCATALYTIC AND ANTIBACTERIAL APPLICATIONS",** is an original work done by me under guidance of **Ms. Minu Pius,** Assistant Professor, Department of Physics and Centre for Research St. Teresa's College (Autonomous), Ernakulam in partial fulfillment for the award of the Degree of Master of Physics, I further declare that this project is not partly or wholly submitted for any other purpose and the data included in the project is collected from various sources and are true to best of my knowledge.

PLACE: Ernakulam

DATE: 13-06-22

FATHIMA NOURIN V A

ACKNOWLEDGEMENT

With immense pleasure, I express my deep sense of gratitude to the great God Almighty without whose divine blessings this work would have been never completed. I express my sincere gratitude towards Ms. Minu Pius, Assistant Professor, Department of Physics and Centre For Research, for her valuable guidance in the formation and successful completion of our study. I owe my sincere thanks to all other teachers and lab assistants for providing the facilities in completing this project and for their helping hands .I sincerely thank my parents for their guidance and support.

ABSTRACT

The project deals with the synthesis of Zinc Ferrite nanoparticles at different calcinations temperatures and characterization to obtain the optimized sample. This sample is made to form nanocomposite with Silver and Silver Chloride. The synthesis of Zinc Ferrite is done by co-precipitation method using chloride precursors and NaOH as precipitating agent. The nanocomposite is made in the same procedure by adding Silver precursors at different stages of synthesis. Thus different samples are obtained the photo catalytic ability and antibacterial ability of the samples is evaluated. The nanocomposite of Zinc ferrites shows a maximum degradation of 98% efficiency which makes them very useful as a photo catalyst. The sample can be retrieved by applying external magnetic field due to the super paramagnetic nature.

The antibacterial properties show that the Zinc Ferrite and silver chloride nanocomposite have higher antibacterial properties. Thus the composite sample has a great potential to be used for targeted drug delivery and antibacterial applications.

The study focuses on the effect of calcination temperature on different samples and the variations in properties due to their different composition.

CONTENTS

CHAPTER 1

1.Introduction..... 1

1.1Ferrite Nanoparticles 1

1.2 Relevance of Zinc Ferrites 2

1.3 Structure of Zinc Ferrites 2

1.4 Synthesis Techniques 3

1.5 Relevance of calcinations temperature in Co-precipitation method 4

1.6 Applications of Zinc Ferrite Nanoparticles 5

1.7 Relevance of Zinc Ferrite Nanocomposites. 5

CHAPTER 2

2. Experimental Methods..... 7

2.1 Synthesis of Zinc Ferrite nanoparticles 7

2.2 Synthesis of Zinc Ferrite nanocomposites 9

2.3 Characterizations 10

2.3.1 X-ray Diffraction (XRD) Studies 10

2.3.2 Fourier Transform Infrared Spectroscopy (FTIR) Studies 12

2.3.3 Thermo gravimetric Analysis and Differential Scanning Calorimetry (TGA and DSC)Studies 13

2.3.4 Vibrating Sample Magnetometer (VSM) Studies) 14

2.3.5 UV-VIS-IR Spectroscopic Studies 15

2.4 Applications 17

2.4.1 Photo catalytic Degradation of Methylene Blue 17

2.4.2 Antibacterial Studies 18

CHAPTER 3

3. RESULTS AND DISCUSSIONS..... 19

3.1 Characterization and Analysis of Zinc Ferrite Nanoparticles 19

3.1.1 XRD Analysis 19

3.1.2 TGA-DSC Analysis 22

3.13 FTIR Analysis 23

3.14 VSM Analysis 25

3.15 UV-VIS-IR Analysis 26

3.2 Applications of Zinc Ferrite Nanoparticles 27

3.2.1 Photo catalytic Degradation of Methylene Blue Dye 27

3.2.2 Retrieval of Photo catalyst 30

3.2.3 Antibacterial Studies 31

3.3 Characterization and Analysis of Zinc Ferrite/AgCl-Ag Nanocomposite 32

3.3.1 XRD Analysis 33

3.2.3 FTIR Analysis 35

3.2.3 VSM Analysis 37

3.4 Applications of Zinc Ferrite Nanocomposites 38

3.4.1 Photo catalytic Degradation of Methylene Blue Dye 38

3.4.2 Antibacterial Studies 42

CHAPTER 4

4. CONCLUSION..... 43

FUTURE SCOPE..... 44

REFERENCES..... 46

CHAPTER 1

INTRODUCTION

1.1 Ferrite Nanoparticles

Ferrite is a type of ceramic compound composed of iron oxide (Fe_2O_3) combined chemically with one or more additional metallic elements. Ferrites are hard, brittle, iron-containing and polycrystalline—i.e., made up of a large number of small crystals. They are composed of iron oxide and one or more other metals in chemical combination. Ferrites can have several different types of crystalline structures, including spinel, garnet, perovskite, and hexagonal. They are ferrimagnetic, meaning they can be magnetized or attracted to a magnet, and are electrically nonconductive. In ferrites the magnetic moments of constituent atoms align themselves in two or three different directions. Ferrites are exceptional magnetic materials that exhibit a strong magnetic property, relatively low conductivity, low eddy current and dielectric losses, and high permeability. Ferrite nanoparticles (FNPs) belong to a broad group of magnetic nanoparticles (MNPs). Ferrite's electrical and magnetic features are influenced by various factors, including the method of preparation, elemental composition, sintering temperature, cation distribution, particle size, etc.

Because of their large surface to volume ratio, ferrite nanoparticles exhibit fascinating and significantly different magnetic properties than those of bulk materials. Ferrite nanoparticles have wide applications in several areas such as biomedical, wastewater treatment, catalyst and electronic device.

In terms of biomedical applications, they are used for diagnosis (magnetic resonance imaging, biosensors), cancer treatment, drug delivery systems, and magnetic hyperthermia.

1.2 Relevance of Zinc Ferrites

Zinc ferrites are a series of synthetic inorganic compounds of zinc and iron (ferrite) with the general formula of $Zn_xFe_{3-x}O_4$. Reducing the particle size of zinc ferrites, from micron to nanometer size, results in a significant change of their properties. Although bulk zinc ferrite is an antiferromagnetic material; when reduced to nanosize, they exhibit super paramagnetic behavior. Zinc ferrite nanoparticles have unique properties such as chemical and thermal stability due to smaller particle size and higher surface area. It exhibits unique structural, opto-electrical, magnetic and photo catalytic activities, and has high electromagnetic performance, mechanical hardness and moderate saturation magnetization.

1.3 Structure of Zinc Ferrites

Zinc ferrites are normal spinel structures which are cubic close-packed oxides with eight tetrahedral and four octahedral sites per formula unit. Zinc ferrite ($ZnFe_2O_4$) possesses an AB_2O_4 structure with tetrahedral A site occupied by Zn^{2+} ions and octahedral B site with Fe^{3+} ions in a face-centered cubic unit cell.

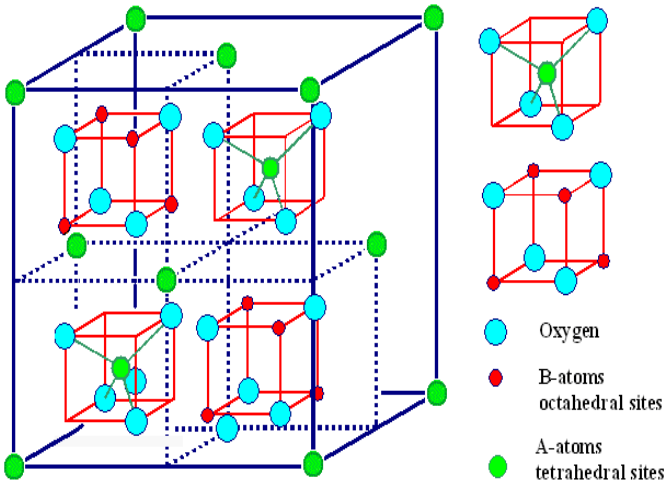

AB_2O_4 spinel The red cubes are also contained in the back half of the unit cell

1.4 Synthesis Techniques

Many methods can be employed for the synthesis of zinc ferrite nanoparticles. The most common among those are sol-gel synthesis and co-precipitation, which are both bottom-up synthesis processes.

Sol-gel synthesis is also known as wet chemical method. The sol-gel method is a conventional and industrial method for the synthesis of nanoparticles with different chemical composition. The basis of the sol-gel method is the production of a homogeneous sol from the precursors and its conversion into a gel. In this method, the molecular precursor is dissolved in water or alcohol and converted to gel by heating and stirring by hydrolysis. The solvent in the gel is then removed from the gel structure and the remaining gel is dried. The properties of the dried gel depend significantly on the drying method. After the drying stage, the produced gels are powdered and then calcined.

Co-precipitation is a phenomenon where a solute that would normally remain dissolved in a solution precipitates out on a carrier that forces it to bind together, rather than remaining dispersed. In the process of co-precipitation, chemical similarities between a carrier and a solute allow the two to bind in some way. The binding pulls the solute out of the solution as the carrier forms crystals or other structures. These can potentially be skimmed out or remove in other ways, leaving a purified solution behind.
There is also biological synthesis method, which involves the use of biological reducing and stabilizing agents such as plant extracts, bacteria, fungi, fruit extracts and natural biopolymer which is safer and safer and environmental friendly. Sono-chemical method and solution combustion method are also some of the synthesis techniques. The solution combustion technique is useful in preparation of high-quality ferrite nanoparticles.

1.5 Relevance of calcination temperature in co-precipitation method

Calcination refers to thermal treatment of a solid chemical compound whereby the compound is raised to high temperature without melting under restricted supply of ambient oxygen for the purpose of removing impurities or volatile substances.

Calcination temperature is the temperature at which calcination is performed. Samples to be studied are calcined at higher temperatures and it is seen that as the calcination temperature is increased, the crystalline nature of the nanoparticles was improved and had an effect on the size and shape of the crystal formed. Calcined materials at higher temperatures, exhibited greater activity as a result of larger particle size and high crystallinity. Calcination temperatures allowed obtaining materials with good optical, morphological and magnetic properties that enable their efficient use in various fields.

1.6 Applications of Zinc Ferrite Nanoparticles

Sl.No.	Title	Application
1	Fabrication and characterization of self-assembled zinc ferrite nanospheres for biomedical applications.(2022)	Biomedical application
2	Zinc ferrite nanoparticles from industrial waste for Se (IV) elimination from wastewater.(2022)	Waste water treatment
3	Biogenic synthesis enhanced structural, morphological, magnetic and optical properties of zinc ferrite nanoparticles for moderate hyperthermia applications.(2021)	Hyperthermia application
4	"Anti-bacterial and wound healing-promoting effects of zinc ferrite nanoparticles(2021)	Antibacterial and wound healing effect

1.7 Relevance of Zinc Ferrite Nanocomposites

Zinc ferrite nanoparticles alone have appreciable properties and applications in different fields but are limited. Zinc ferrite nanocomposites are used in order to enhance the properties, enabling it for more applications.

Sl.No.	Title	Application
1	Eco-friendly synthesis of cobalt-zinc ferrites using quince extract for adsorption and catalytic applications: An approach towards environmental remediation. (2022)	Adsorptive removal of pollutants, catalytic decomposition of the H_2O_2 and low-frequency hyperthermia.
2	Controllable synthesis of zinc ferrite nanostructure with tunable morphology on polyaniline nanocomposite for super capacitor application. (2022)	Various applications from electronic devices to transportation.
3	Modulation of magneto electric coupling through systematically engineered spin canting in nickel–zinc ferrite (2022).	Used in modulation of the Magneto Electro coupling in spinel-structured oxides.
4	Recent advances on synthesis, characterization and high frequency applications of Ni-Zn (ferrite nano particles. (2021)	Microwave devices, power transformers in electronics, rod antennas

CHAPTER 2

EXPERIMENTAL METHODS

In the present study, Zinc Ferrite nanoparticles and composite of silver and silver chloride with Zinc Ferrite nanoparticles are synthesized by co-precipitation method and the temperature dependence on the properties are evaluated. The co-precipitation technique is a promising method to synthesize easily reproducible and pure nanomaterials at low temperature and low cost.

2.1 Synthesis of Zinc Ferrite Nano Particles

The Nano particles of Zinc Ferrites are synthesized using chloride precursors and sodium hydroxide as precipitating agent at room temperature and subsequent precipitate is subjected to calcinations over a temperature range of 100 to 800^{O}C.

$$2\ FeCl_3.6H_2O + ZnCl_2 + 8\ NaOH \rightarrow ZnFe_2O4 + 8NaCl + 10\ H_2O$$

(Chloride precursors)

Ferric Chloride hexahydrate ($FeCl_3.6H_2O$), Zinc Chloride ($ZnCl_2$) and sodium hydroxide (NaOH) combined in the stoichiometric ratio 2:1:8 to form Zinc Ferrite ($ZnFe_2O4$), Sodium Chloride (NaCl) and water (H_2O).

Optimized concentration:

$$FeCl_3.6H_2O : ZnCl_2 : NaOH = 0.1M : 0.05M : 0.4M$$

The required weight of salts are found using the formula,

$$W = \frac{(\boldsymbol{Molecular\ mass}\ (\boldsymbol{u}) \times \boldsymbol{Volume}\ (\boldsymbol{ml}) \times \boldsymbol{Molar\ concentration}\ (\boldsymbol{M}))}{1000(ml)}$$

Sl. No.	Compound	Molecular mass(u)	Volume (ml)	Molar Concentration (M)	Required Weight (g)
1	$FeCl_3.6H_2O$	270.3	300	0.1	8.109
2	$ZnCl_2$	136.28	300	0.05	2.044
3	NaOH	40	600	0.4	9.6

The required weights are measured using electronic balance. The Ferric chloride, Zinc Chloride, NaOHpowders are stirred in distilled water for half hour. The precipitating agent NaOH are added dropwise into this mixed solution of ferric chloride and zinc chloride subjected to constant magnetic stirring at a temperature of 80^{O}C. After 2 hours the precipitation begins. The pH of the mixture should be 10-12 range. The solution is kept in a hydrothermal unit at a temperature of 100^{O}C for 90 minutes for digestion. The obtained precipitate is washed with distilled water and acetone and centrifuged at a rate of 6000 rpm, 3-4 times. This sample is kept for drying for 2 hours. Then the sample is grinded for 30 minutes in a mortar and pestle. The powdered precipitate is subjected to calcinations at a temperature range of 100 to 800^{O}C in a muffle furnace for 6 hours for obtaining different samples ZF100, ZF200, ZF300.....ZF800. The calcined and uncalcined samples are characterized using different techniques and optimized sample is chosen for composite synthesis.

2.2 Synthesis of Zinc Ferrite nanocomposites

The composite with silver and silver chloride are prepared by combining the optimized sample of Zinc ferrite nanoparticles with silver nitrate ($AgNO_3$) and trisodium citrate (TSC).

Optimized concentration: ***AgNO3: TSC = 0.01M: 0.1M***

Sl. No.	Compound	Molecular mass(u)	Volume (ml)	Molar Concentration (M)	Required Weight (g)
1	$FeCl_3.6H_2O$	270.3	200	0.1	5.406
2	$ZnCl_2$	136.28	200	0.05	1.363
3	NaOH	40	500	0.4	8
4	$AgNO_3$	169.87	350	0.01	0.595
5	TSC	294.1	350	0.1	10.294

The synthesis procedure of Zinc ferrite is done as discussed above and the silver nitrate and trisodium citrate mixture is added at different stages of precipitation for obtaining different samples. Calcination is done by keeping the samples taken in crucibles in muffle furnace for 6 hours.

a) Slow mixing of silver nitrate and trisodium citrate with the precipitate of Zinc Ferrite sample. Calcination at temperature 500^oC - 800^oC. Samples obtained are labeled as CS500, CS600, CS700, and CS800.

b) Sudden mixing of silver nitrate and trisodium citrate after the precipitate is formed. Calcination at 700^OC and sample is CS1.

c) Mixing of silver precursor is done after centrifugation of zinc ferrite precipitate. Samples are calcined at temperature of $700^{O}C$. Sample is named as CS2.

2.3 Characterizations

The structural, optical, thermal and magnetic characterizations of the zinc ferrite nanoparticles and nanocomposite samples are done and the properties are compared.

2.3.1 X-ray Diffraction (XRD) Analysis

X-ray diffraction techniques are used to study the structure of solids and crystalline materials. The crystalline nature, the chemical composition, lattice parameters, crystallite size etc., can be obtained from the XRD data. This method involves the elastic scattering of an X-ray beam from a sample and the intensity of the beam as a function of scattered angle is studied.

The most common methods in X-ray diffraction are the powder diffraction method. In this method the X-ray diffraction on powder or microcrystalline samples are used for structural characterization of materials using a powder diffract meter.

The sample contains a large number of crystallites or grains with random orientations. When a monochromatic beam falls upon the atoms in the Bragg's plane scattered radiations will emerge from each atom in all directions. Strong amplification of emitted signal occurs at very specific angles, where the scattered waves interfere constructively. This effect is called diffraction. The angle between the incident and scattered beam is 2θ.

Constructive interference takes place when the Bragg's law is satisfied, i.e.

$$2dsin\theta = n\lambda \qquad (2.1)$$

Where n is the integer describing the order of reflection, λ is the wavelength of radiation and d is the interplanar spacing.

X-ray diffraction pattern

XRD pattern is a plot of intensity of the radiations over the y axis and angle between incident and scattered radiation on the x axis. The peaks shown in the plot depicts the structure of the sample. The appearance of broad peaks implies the amorphous nature of material and short range order, whereas the sharp peaks is due to crystalline nature of the material. The lattice parameters, interplanar spacing, crystallite size can be calculated by knowing the miller indices corresponding to each peak. The structure of the sample is determined from the lattice parameters.

The crystallite size D can be calculated using Debye-Scherer equation;

$$D = \frac{0.94\,\lambda}{B cos\theta}. \qquad (2.2)$$

Where B and θ represents the full width at half maximum and diffraction angle respectively.

XRD is one of the widely used tools for the structural characterization of nanomaterials of any sizes. The observed change in position of diffraction peaks of each sample gives the variations of crystalline structure and parameters.

2.3.2 Fourier Transform Infrared (FTIR) Studies

FTIR spectroscopy is a disperse method, where measurements are performed over a broad spectrum instead of a narrow band of frequencies. It is a spectroscopic method used to evaluate the chemical bonds in a material by producing infra-red absorption spectrum. The infrared radiations interact with the molecules changing the dipole moment causing vibrations. The vibrations can induce stretching, contraction, or bending in the sample. These results in the absorption of infra-red radiation over a specific wave number range and the absorbed radiations are recorded. The correlation between bond wave number and position with chemical structure is used to identify the functional groups of a material.

The FTIR system consists of the source that produces the infra-red radiations, followed by interferometer, and detector. Spectrometer obtain infrared spectrum by collecting the interferogram of a sample signal with an interferometer, which measures all the infrared frequencies simultaneously transmitted or reflected from sample surface. The beam arrives at the detector and is measured by the detector. These detected interferogram are decoded by a computer with a mathematical technique in terms of Fourier Transform and spectrum is produced.

FTIR spectrum consists of transmittance or absorbance and wave number dependence. Generally a wave number range of 400 – 4000 cm^{-1} is analyzed. The finger print regions in the spectrum are unique for a material and can be used to distinguish between compounds.

FTIR spectroscopy can be used for quantitative and qualitative analyze of solid, liquid or gaseous samples, without destroying the sample. This method is applicable to organic or inorganic materials.

2.3.3 TGA and DSC

Thermal analysis describes the techniques which are used to analyze the changes occurring in a substance when it is heated o cooled. This method consists of different methods, which are distinguished from one another by the property which are being measured.

Thermo Gravimetric Analysis (TGA)

TGA is a technique by which the mass of a given sample is monitored as a function of time or temperature as the sample specimen is subjected to a controlled temperature. The analysis is performed using TG analyzer. This consists of a sample pan where the sample is taken supported by a precision balance. This setup measures the weight of the sample throughout the experiment. A sample purge gas controls the sample environment.

The TGA curve is a plot describing time or temperature along the abscissa and Weight loss or weight along y axis. The change in sample composition, thermal stability, Oxidative properties, and Volatile content of the material can be determined from TGA curve.

Differential Scanning Calorimetry (DSC)

The difference in heat flow rate between a sample and inert reference as a function of time and temperature is measured. DSC gives the information of heat flow into and out of the sample.

The heat flows into the sample as a result of heat capacity (heating), melting, evaporation, endothermic process etc. and heat flows out of the sample as a result of heat capacity (cooling), crystallization, oxidation and exothermic processes.

Heat from heater is supplied to the sample and the reference through heat sink and heat resistor. Heat sink has enough heat capacity compared to the sample. In case the sample occurs endothermic or exothermic phenomena such as transitions and reactions these are compensated by the heat sink, keeping the temperature difference between sample and reference constant.

The DSC curve displays the time or temperature along x axis and heat flow rate along y axis. The peaks in the curve represent endothermic and exothermic processes.

DSC curve measures enthalpy change, compensates heat release or absorbed during thermal event, oxidation of the sample etc.

Simultaneous DSC – TGA Curve (SDT)

SDT measures both heat flow and weight loss of a material as a function of temperature or time in a controlled atmosphere. Thus productivity is increased and interpretation of the results is simplified.

This provides information about endothermic and exothermic processes which are having no associated weight loss and which involve weight loss respectively.

2.3.4 Vibrating Sample Magnetometer (VSM) Studies

The magnetic properties of the samples are analyzed by using Vibrating Sample Magnetometer which operates on the Faraday's Law of Induction. Faraday's law states that a change in magnetic field will create an electric field, and by measuring the electric field the changing magnetic field can be analyzed. VSM studies provide information about the magnetic behavior of materials.

The sample is subjected to a constant magnetic field, which causes the magnetization inside the material to be polarized. So that, the material can generates the magnetic field by itself even after the removal of external magnetic field. Then the sample is made to vibrate in an alternating magnetic field, this variation in the magnetic field will produce an electric field. This induces current in the coil which can be measured to determine the magnetization of the material.

VSM studies indicate whether the materials can be magnetized, the nature of magnetism exhibited and the extent of magnetization the sample.

The VSM data can be used to study the hysteresis by drawing the M-H curve. The M-H curve represents magnetic field along the x-axis and the magnetization along the y axis. The hysteresis of the curve determines the type of magnetism exhibited by the sample.

2.3.5 Ultra Violet and Visible (UV –VIS) Spectroscopic Studies.

UV – VIS spectroscopy is a spectroscopic method which studies the optical characteristics of a material. UV-VIS spectroscopy performs optical spectroscopy. This method involves the interaction of light with matter in the ultraviolet and visible region.

When a material is irradiated with a beam of radiations, the particles absorb energy to excite into higher energy levels which results in the loss of energy by a certain amount. The variation of intensity is recorded by the detector. The material only absorbs certain wave lengths, the measured absorbance or transmittance gives information about the optical characteristics.

The instrument used is known as spectrophotometer. The source produces radiations of wavelength 200-800 nm, which is passed to a monochromater which separates all the wavelengths of the beam into single beam. The beam separator separates the beam and guide into two directions. There will be two cuvettes made of quartz or glass which consists of sample and reference solution. The change in intensity of radiation of the sample is compared with the reference. Both of these are connected to a detector. This measures the light passing through the sample and compares it to the intensity of light before it passes through the sample. The ratio is called the transmittance ratio. The spectrophotometer can be configured to measure the reflectance also. The transmittance or reflectance with wavelength is recorded and spectrum is obtained.

The spectrum consists of wavelength along x axis and absorbance along y axis. The wavelength at maximum absorption bands will give information about the structure of molecule or ion, and the extent of absorption is proportional with the amount of species absorbing the light.

The amount of light absorbed and concentration of the sample has a linear relation explained by Beer – Lambert's law.

$$A = log_{10}(I_0/I) = \varepsilon.c.L \qquad (2.3)$$

Where A is the measured absorbance, I_o and I are the intensities of incident and transmitted beams, L is the path length through the sample and c is the concentration. ε is the molar absorptivity or extinction coefficient.As the concentration increased the absorption also increases.

A tauc plot is drawn with x axis representing hν and $(\alpha h\nu)^2$ along y axis, where $\alpha$is the absorption coefficient. The value of exponent is determined by the type of transition. The value 2 implies direct transitions. The plot follows a linear regime over a specific range, which marks the onset of

absorption. By extrapolating this linear region on the x axis, the band gap can be determined.

2.4 Applications

2.4.1. Photo catalytic Degradation of Methylene Blue

The chemical name of methylene blue is Methylthioninium Chloride, which is used as a dye and as a medication. It is a cationic dye. This is used to stain cells in biological applications, paints, textiles etc. The heavy dose of methylene blue is highly toxic. Based on recent studies it has a high potential to become carcinogenic. The dye is expected to be significantly bio accumulate.

The degradation of dye is done using photo catalysis. Photo catalysis is a chemical process that takes place in the presence of light with the activity of a photo catalyst. This method is employed for the complete degradation of pollutants or chemicals which are harmful and cause pollution. The ability of the sample to degrade the dye in presence of sunlight is studied with time. The degradation efficiency is calculated and compared with the different samples.

The dye in the presence of synthesized samples is subjected to sunlight exposure for a period of 4 hours. 3 ml of the solution is taken after every 30 minutes and the variation of absorbance spectrum of the methylene blue dye is studied using UV-VIS-NIR Spectrophotometer. The degradation efficiency is calculated by knowing the maximum value of absorbance of dye kept at dark and that of the sample.

$$Degradationefficiency\ (\%) = \frac{C_0 - C_s}{C_0} x100 \qquad (2.4)$$

Where C0 and CS represents the maximum value of absorbance of dye in dark and sample in sunlight.

2.4.2 Antibacterial Studies

Antibacterial activity is the potential for inhibiting the growth of bacteria. Antibacterial activity is the most important phenomenon which gives adequate protection against microorganisms**.** The antibacterial property of the sample is studied by well diffusion method for both gram positive and gram negative bacteria.

The agar medium is prepared on a sterile glass petri plates and solidified then swabbed using sterile cotton with reference bacterial strain. These agar plates are punched using sterile tips of sample dispersed in water via sonification and poured with a micropipette. These plates are allowed to stand for some time and were incubated. The zone of inhibition is measured. The measured zone of inhibition determines the antibacterial properties of the sample .

CHAPTER 3

RESULTS AND DISCUSSIONS

3.1 Characterization and Analysis of Zinc Ferrite Nanoparticles

Sample	Calcination Temperature (^{O}C)
ZF Unc	Uncalcined
ZF100	100
ZF200	200
ZF300	300
ZF400	400
ZF500	500
ZF600	600
ZF700	700
ZF800	800

3.1.1 X-Ray Diffraction (XRD) Analysis

The samples of Zinc Ferrite Nanoparticles are characterized using X-ray diffraction (XRD) studies.XRD pattern are obtained using AXS D8 Advance X-ray diffractometer with Cu-Kα radiation (λ=1.5406 A^{O}) scanning in the range 2θ = 10-80^{O}. The X- ray generator is operated at 40kV and 35mA.

The structure and size of Zinc Ferrite nanoparticles are determined from the XRD pattern. The crystal structure of Nanoparticles is compared with the JCPDS file. For cubic structure, the lattice constants are equal, a=b=c.

The XRD pattern for the different samples are obtained as shown in figure 3.1 The emergence of the peaks can be seen for the samples calcined at $400^{O}$and above. Thus the crystallization of the Zinc Ferrite nanoparticles takes place around 400^{O}C and the most intense peak (311) is obtained for the sample calcined at 800^{O}C. Therefore the crystalline growth is favored with increase in temperature.

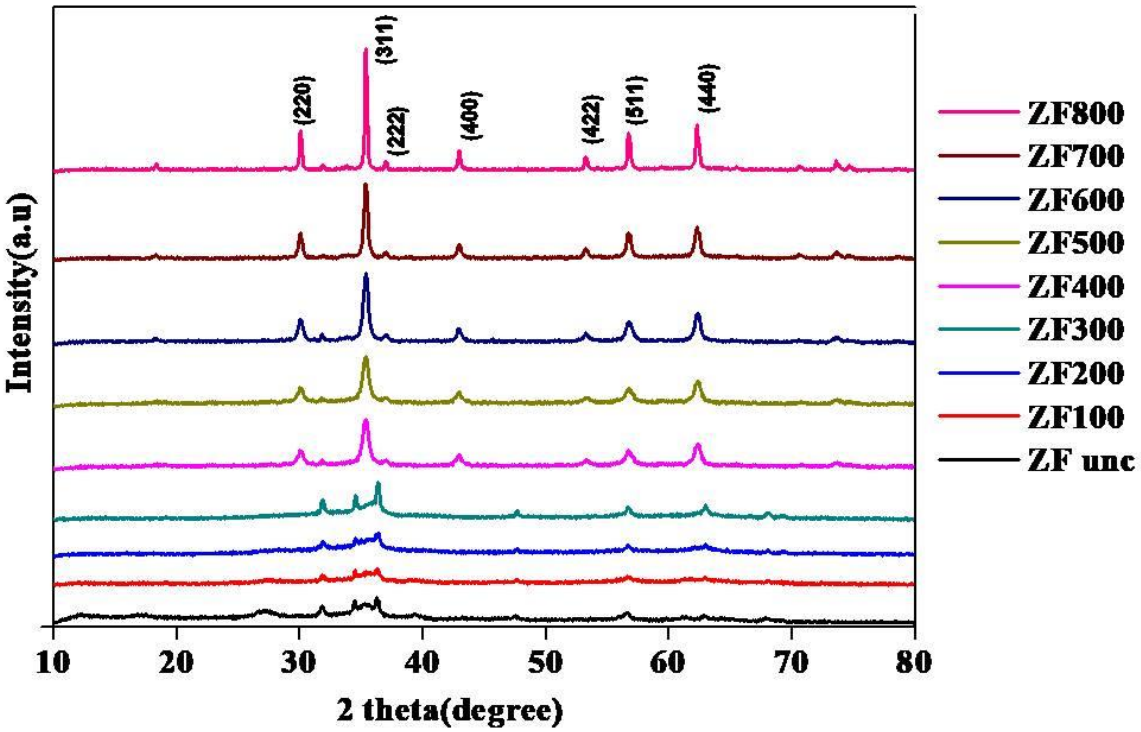

Figure 3.1 XRD patterns of Zinc Ferrite nanoparticles at different calcination temperature

The characteristic peaks are obtained at 2θ values 30.047^{o}, 35.384^{o}, 42.968^{o}, 53.25^{o}, 56.6^{o} and 62.285^{o} corresponding to the reflection planes (220),(311),(400), (422),(511) and(440) respectively. The most intense peak is obtained for the 311 plane (35.384^{O}). These peaks matches with the JCPDS(Card No.82-1049), confirming the formation of spinel cubic structure with the Fd3m space group, with lattice constant a = 8.441 A^{O}. The sharp and well defined peaks indicate the formation of Zinc Ferrite

nanoparticles and crystallinity for the samples ZF400-ZF800. The increase in intensity can be attributed to the increased crystallite size.

The crystallite size was calculated using Debye -Scherer equation and are tabulated. The crystallite size varies from 15.16 nm to 38.78 nm. The crystallite size is found to increase with temperature and maximum value is obtained for ZF800.

The lattice parameter values are consistent with the single-crystalline cubic spinel form of Zinc Ferrite Nanoparticles. The absence of any other peaks implies the phase purity of the sample.

Table 3.1 the crystallite size and lattice parameters corresponding to the reflecting plane (311)

Sample	Diffracting Angle (2θ°)	β (rad)	Crystallite size D(nm)	Interplanar spacing D (A°)	Lattice constant a (A°)
ZF400	**35.333**	**0.00878**	**16.58**	**2.53823**	**8.418**
ZF500	**35.327**	**0.0096**	**15.16**	**2.53865**	**8.420**
ZF600	**35.362**	**0.00808**	**18.01**	**2.53623**	**8.412**
ZF700	**35.338**	**0.0062**	**23.49**	**2.5379**	**8.417**
ZF800	**35.352**	**0.00375**	**38.78**	**2.53694**	**8.414**

3.1.2 Thermo gravimetric Analysis And Differential Scanning Calorimetry (TGA –DSC) Analysis

The thermal properties of the uncalcined samples are analyzed using TGA-DSC method. TGA curve indicates the beginning of weight loss at a temperature around 42^{O}C. The weight loss is calculated as a function of temperature over a range of temperature 0^{O}C to750^{O}C. The maximum weight loss is about 22%.

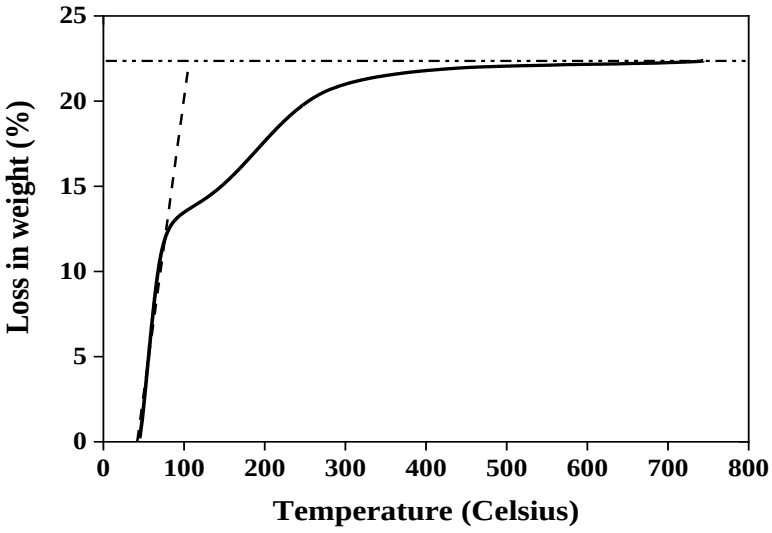

Figure 3.2 Weight loss curve of uncalcined Sample.

The weight loss can be seen from temperature of 77^{O}C to 130^{O}due to the desorption of water, in the sample, the corresponding endothermic curve is obtained at 82.5^{O}C.

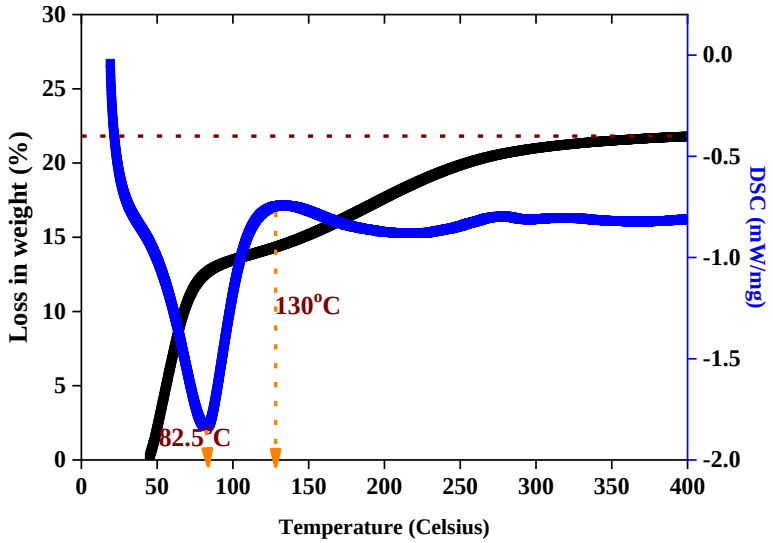

The weight loss from 130^{O}C to 300^{O}C is arising due to the decomposition of Iron and Zinc hydroxides. From 400^{O}C to 700^{O}C no significant weight can be seen, stating the thermal stability of the material.

3.1.3 Fourier Transform Infrared Spectroscopy (FTIR) Analysis

The FTIR studies are conducted for the samples using Fourier transform infrared Spectrometer (thermo Nicolet, Avatar 370) in the range 400 to 4000 cm^{-1}. The FTIR spectrum reveals the characteristic peaks at 400.5 cm^{-1} and 533 cm^{-1} for the samples from ZF400 to ZF800. These two peaks corresponds to the metal oxide vibrations along octahedral (Fe-O) and (ZnO) tetrahedral sites respectively. There is a weak band around 1400 cm^{-1} for samples ZF100 – ZF300 that corresponds to the bending of the –OH bonds. This indicates the presence of feeble water content in these samples.

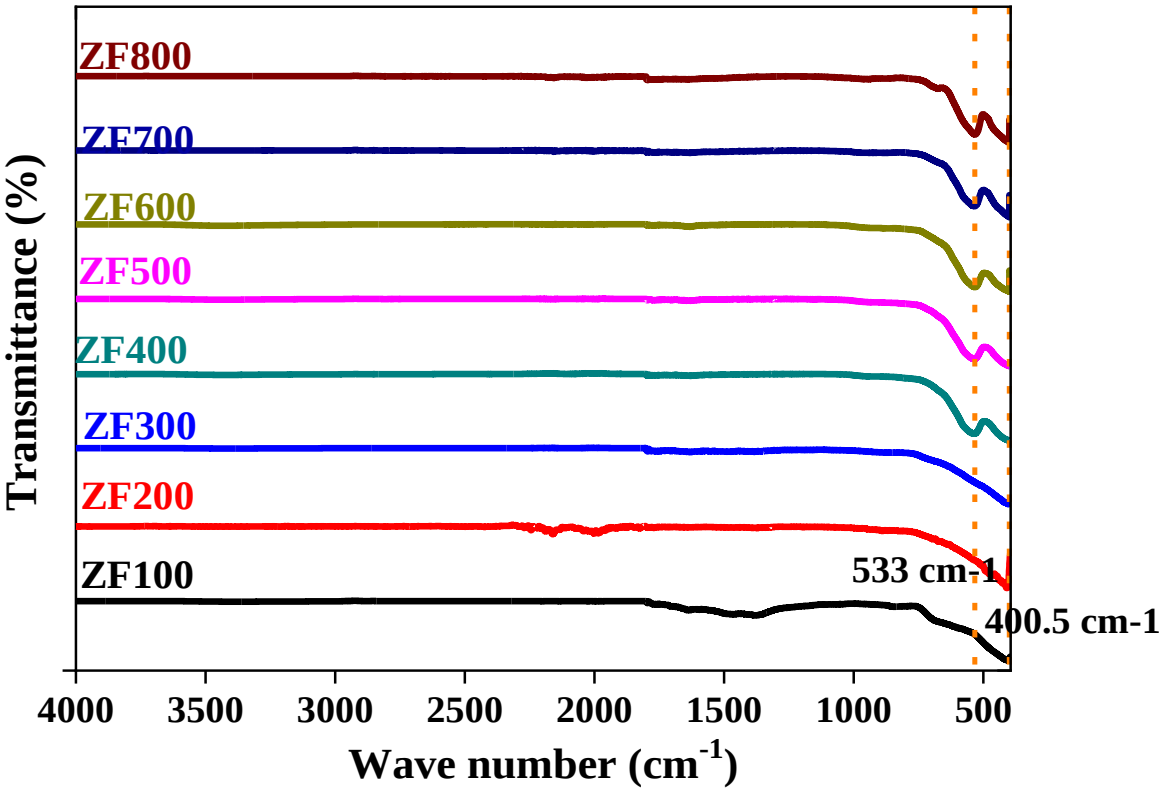

Figure 3.4 FTIR spectrum of different Samples

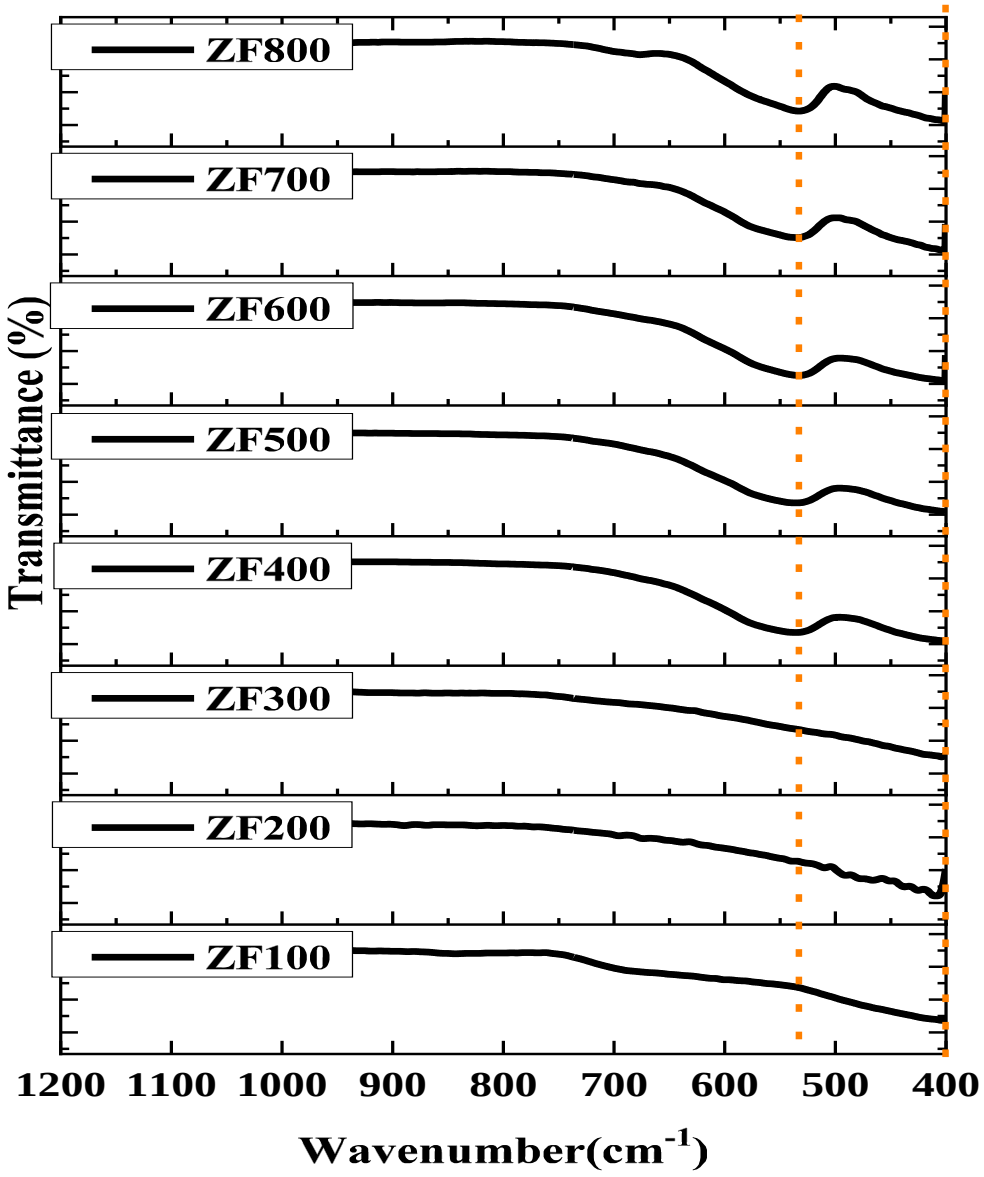

Figure 3.5 FTIR Spectrum showing shift in peaks

3.1.4 Vibrating sample Magnetometer (VSM) Analysis

The magnetic properties of the samples are determined by Vibrating Sample Magnetometer (Lakeshore VSM 7410) at room temperature with an applied. The MH curve, reveals that the samples, ZF400 – ZF800 are having super paramagnetic nature. The characteristic S shaped curve for super paramagnetism is more pronounced for ZF800. The least squareness ratio indicates the formation of single domain particles. Thus the magnetic materials can be retrieved by applying magnetic field. field of -15k – 15kOe.

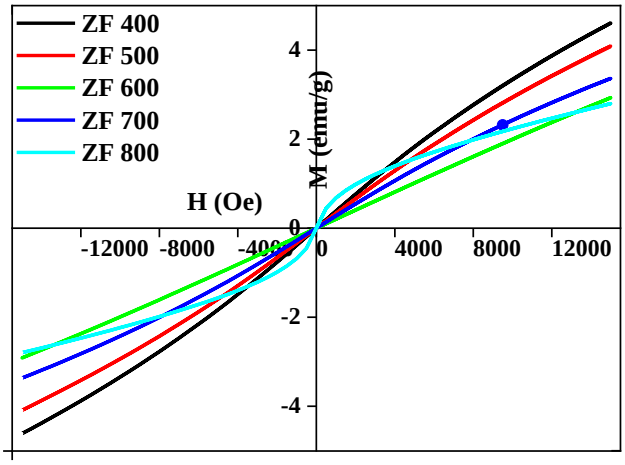

Figure 3.6 M-H curve for ZF Nanoparticles

Sample	Ms (emu/g)	Mr (emu/g)	Squareness ratio(Mr/Ms)
ZF400	4.612	5.18E-05	1.12E-05
ZF500	4.091	1.76E-04	4.31E-05
ZF600	2.923	7.23E-05	2.47E-05
ZF700	3.3666	1.93E-04	5.72E-05
ZF800	2.798	5.33E-05	1.90E-05

3.1.5 UV-VIS-NIR Analysis

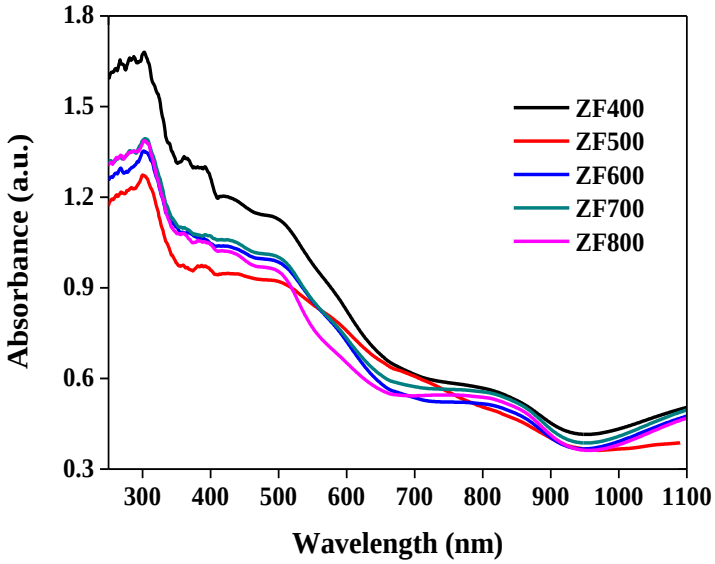

Figure 3.7Absorption spectrum of Zinc Ferrite nanoparticles

The UV-VIS-NIR absorption studies are conducted using Cary 5000 UV-VIS-IR absorption spectrophotometer in the spectral range 220-1980 nm. The maximum absorption is shown by sample ZF400. The range of maximum absorption is about 300nm for all samples. There is a red shift in absorption edge with an increase in calcination temperature which is expected for an increase in crystallite size. Zinc ferrite nanoparticles are found to exhibit direct band gap. Band gap ranges from 1.67 to 1.78 eV. The least band gap is obtained for sample calcined at 500^{O}C

Table3.8 Band gap of ZF Nanoparticles.

Sample	Band Gap
ZF400	1.78
ZF500	1.67
ZF600	1.72
ZF700	1.75
ZF800	1.74

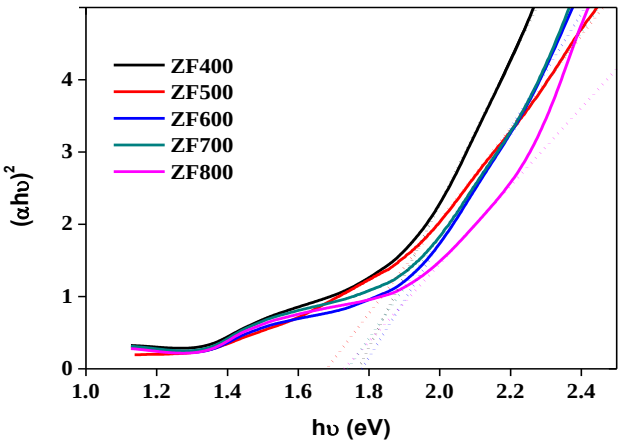

Figure 3.8 Tauc Plot of ZF Namoparticles

3.2 Applications Of Zinc Ferrite Nanoparticles

3.2.1 Photo catalytic Degradation Of Methylene Blue Dye

The different samples were tested for degradation of methylene blue dye (10ppm) in darkness for 15 minutes and 4 hours in sunlight. Dosage of samples used as photo catalyst was 1g/L.

The absorption spectrum of each of the samples is taken for every 30 minute interval for about 3 hours.

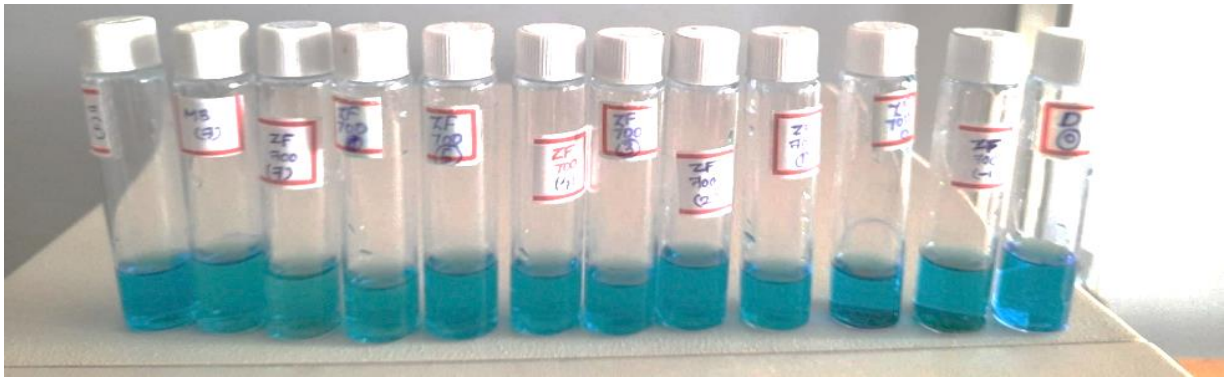

Figure 3.9The sample ZF700 at different time of sunlight exposure in the order D(7),MB(7),ZF700(7),ZF700(6), ZF700(5), ZF700(4), ZF700(3)……..ZF700(0), D(0)

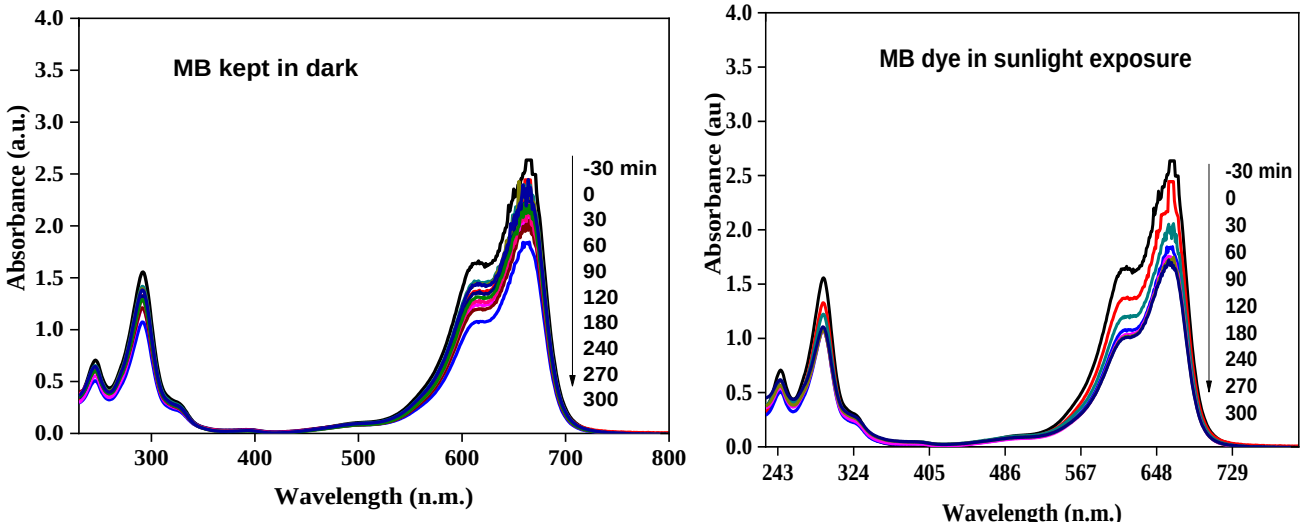

Figure 3.10 Absorption of Dye in dark and in sunlight at different time intervals

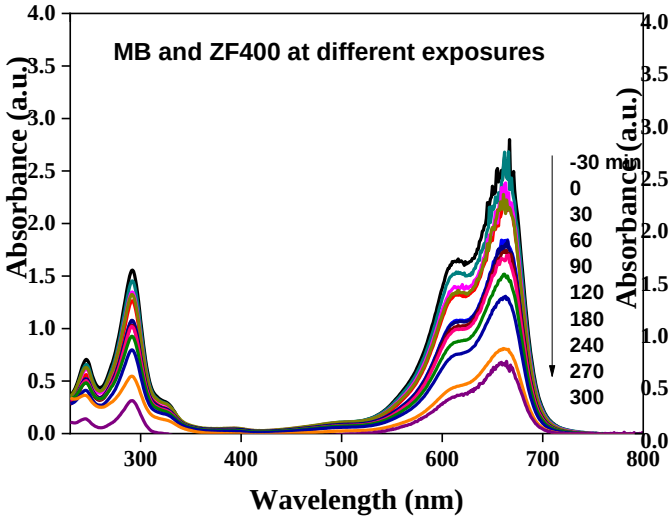
MB and ZF400 at different exposures
Absorbance (a.u.)
Wavelength (nm)
-30 min
0
30
60
90
120
180
240
270
300

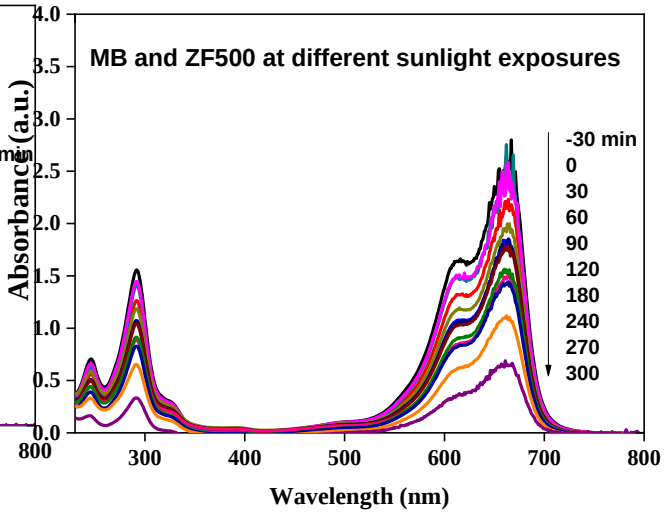
MB and ZF500 at different sunlight exposures
Absorbance (a.u.)
Wavelength (nm)
-30 min
0
30
60
90
120
180
240
270
300

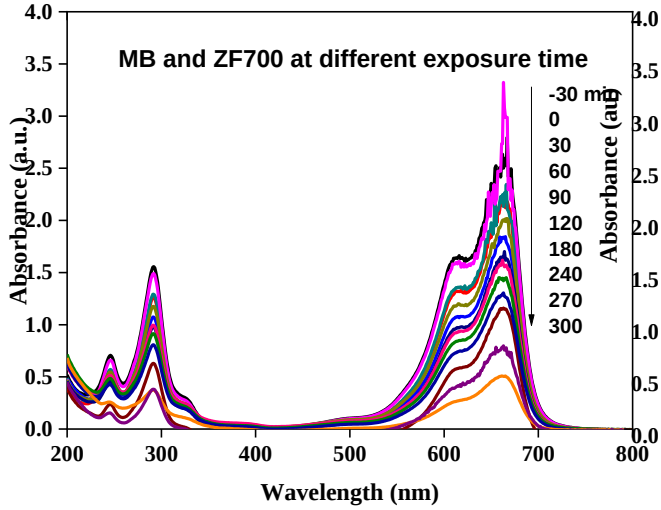
MB and ZF700 at different exposure time
Absorbance (a.u.)
Wavelength (nm)
-30 min
0
30
60
90
120
180
240
270
300

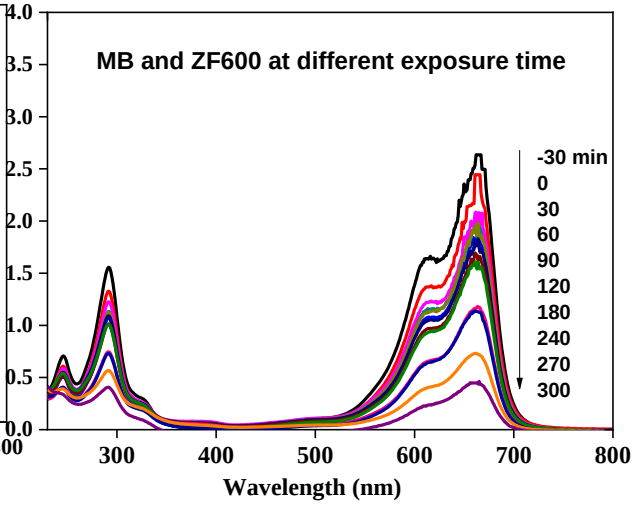
MB and ZF600 at different exposure time
Absorbance (au)
Wavelength (nm)
-30 min
0
30
60
90
120
180
240
270
300

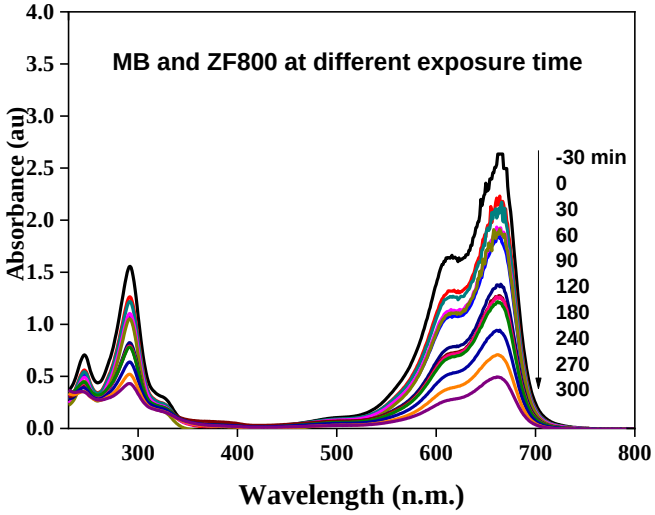
MB and ZF800 at different exposure time
Absorbance (au)
Wavelength (n.m.)
-30 min
0
30
60
90
120
180
240
270
300

The maximum absorption peak wavelength of Methylene blue is about 664 nm. The degradation of dye by different samples for a time period of 4 hours was studied. The maximum degradation was observed with ZF800 about 2 hours exposure to sunlight marked as sample set 4 – ZF800(4).

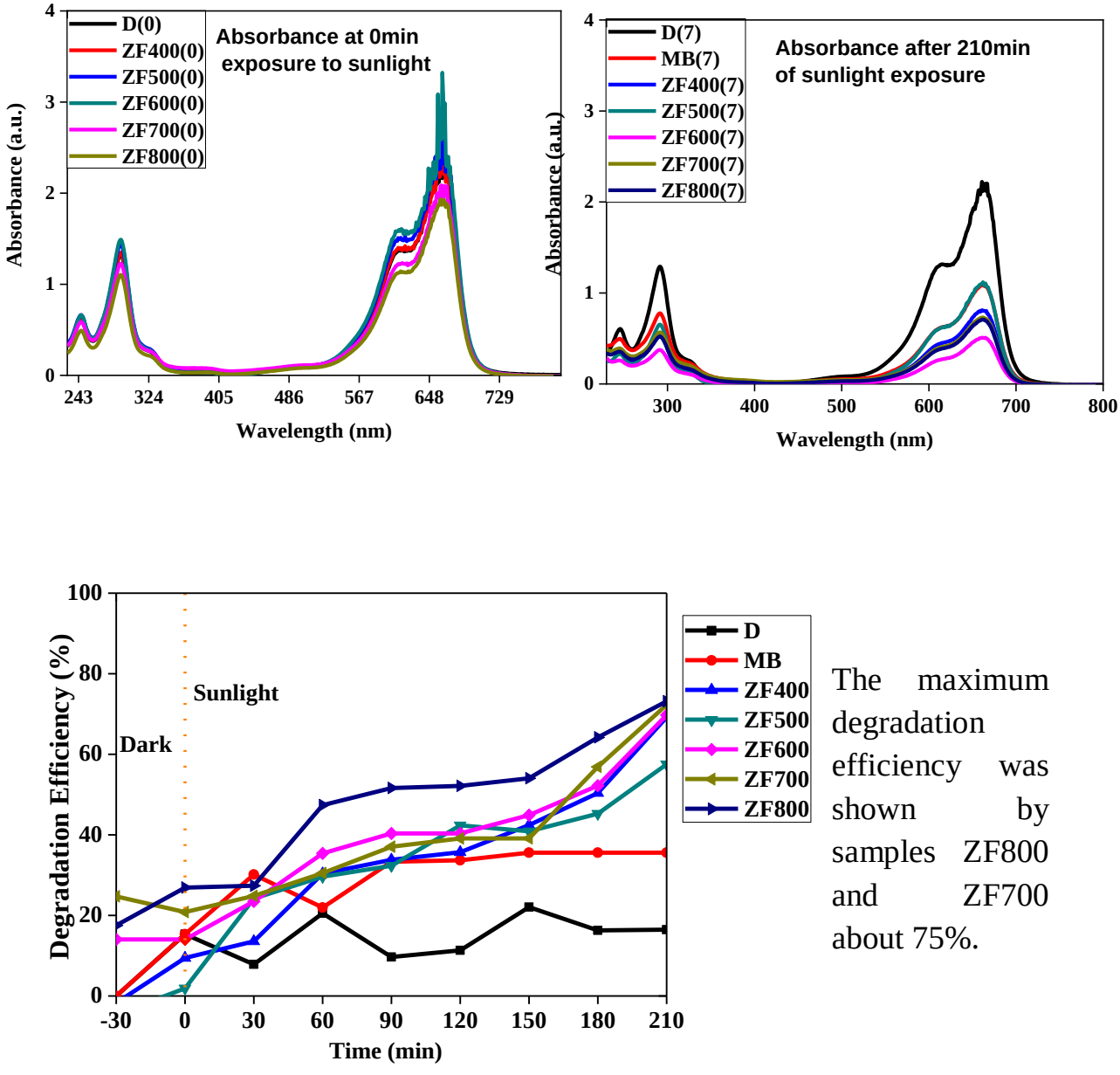

The maximum degradation efficiency was shown by samples ZF800 and ZF700 about 75%.

Figure 3.11Degradation Efficiency of Zinc Ferrite Nanoparticles

During a period of 210 minutes, the absorbance decreases considerably for all the samples. The absorbance is minimum for the sample ZF800. This ability to degrade the dye makes it useful as a photo catalyst.

3.2.2 Retrieval of Photo catalyst

The samples of Zinc Ferrite nanoparticles can be retrieved after photo degradation by applying external magnetic field. This is due to the super paramagnetic nature of Zinc Ferrite nanoparticles. The samples retrieved are again characterized by XRD, no significant change in crystallite size and properties are observed.

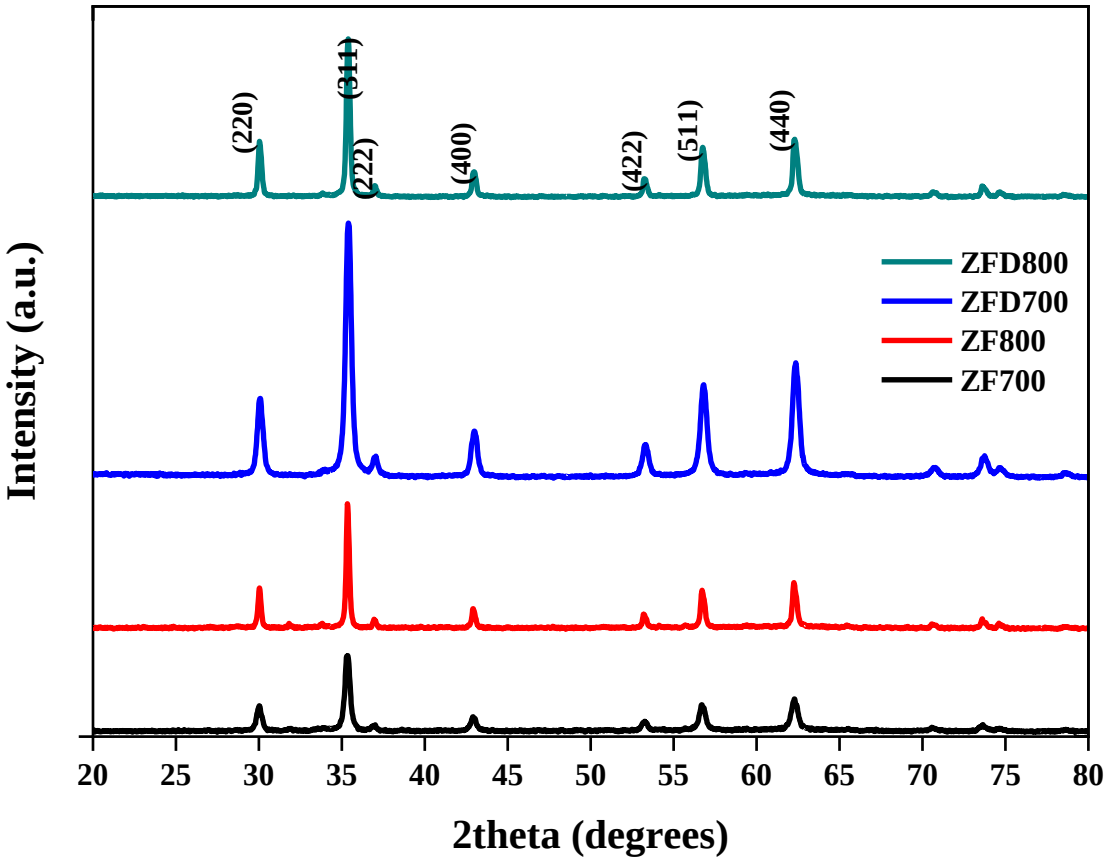

3.2.3 Antibacterial Studies

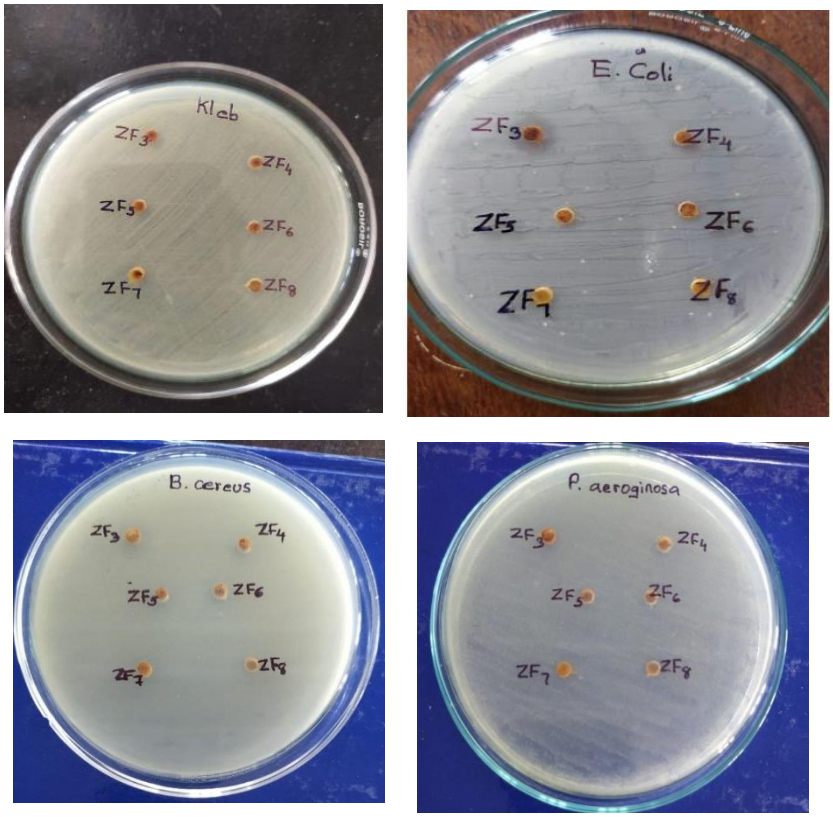

Antibacterial studies are conducted for zinc ferrite nanoparticles using gram positive (Staph.Suereus, Enterococcus, Bacillus) and gram negative bacteria (E.coli, Klebscella p, Pseudomonas) using Well diffusion methods. Only the sample ZF800 shows antibacterial activity against Enterococcus with a zone of inhibition 5 mm. No significant antibacterial activity was shown by the other samples. So, the Zinc Ferrite nanoparticles have no considerable antibacterial properties.

3.3 Characterization and Analysis Of Zinc Ferrite/AgCl-Ag Nanocomposites

Samples	Calcination temperature (°C)	Addition of silver precursors	Addition time
CS 700	700	Drop by drop	After precipitation
CS 800	800	Drop by drop	After precipitation
CS 1	700	Rapid	After precipitation
CS 2	700	Rapid	After centrifugation

3.3.1 X-Ray Diffraction (XRD) Analysis

The structure and size of Zinc Ferrite Composites are determined from the XRD spectrum. The XRD pattern for the different samples is obtained as shown in figure 3.11. The characteristic peak (311) corresponding to Zinc Ferrite nanoparticles is the most intense peak in all samples. This peak has a maximum intensity for sample CS800, suggesting more crystalline nature.

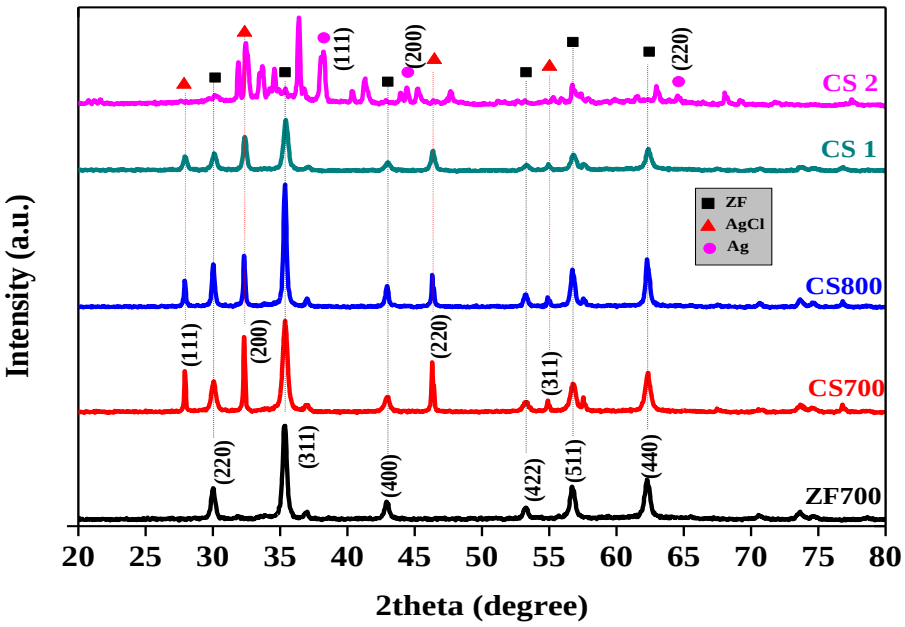

Figure 3.11 XRD Pattern of ZF/AgCl-Ag

The samples CS1,CS700, and CS800 have peaks corresponding to the reflecting planes (111), (200), and (220). These data indicates that the sample CS1, CS700 and CS800 are Zinc Ferrite and Silver Chloride nanocomposites. This is verified with the JCPDS File No:01-071-5209.This represents Fm-3m (225) lattice space group with lattice constant 5.54630 Å.

The Sample CS2 has the peaks corresponding to Silver. This is in agreement with JCPDS File No: 00-004-0783. Thus the sample CS2 is Zinc ferrite and Silver nanocomposite. The space group is Fm-3m (225) and 4.08620 $A^{O}$is the lattice parameter.

Table 3.4 Crystallite size and Lattice Parameter for nanocomposites

Sample	ZF (311)		AgCl (200)		Ag(111)	
	D(nm)	a (A^{O})	D(nm)	a (A^{O})	D(nm)	a (A^{O})
CS700	20.39	8.408	-	-	-	
CS800	31.95	8.4	51.06	5.534	-	-
CS1	21.95	8.39	50.57	5.53	-	-
CS2	42.23	8.1819	30.87	5.528	-	-
ZF700	23.49	8.417	24.55	5.5107	41.96	4.0813

The sample CS2 has got maximum crystallite size and this corresponds to Zinc Ferrite and Silver nanocomposite.

3.3.2 Fourier Transform Infrared Spectroscopy (FTIR) Analysis

The FTIR spectrum reveals the characteristic peaks at 400.5 cm^{-1} and 533 cm^{-1} for the all the composite samples. These two peaks corresponds to the metal oxide vibrations along octahedral (Fe-O) and (ZnO) tetrahedral sites respectively. In addition to these peaks there are peaks at vibrational frequencies 636cm^{-1},865 cm^{-1}, 1451 cm^{-1}, 2974 cm^{-1} and 3420 cm^{-1}.

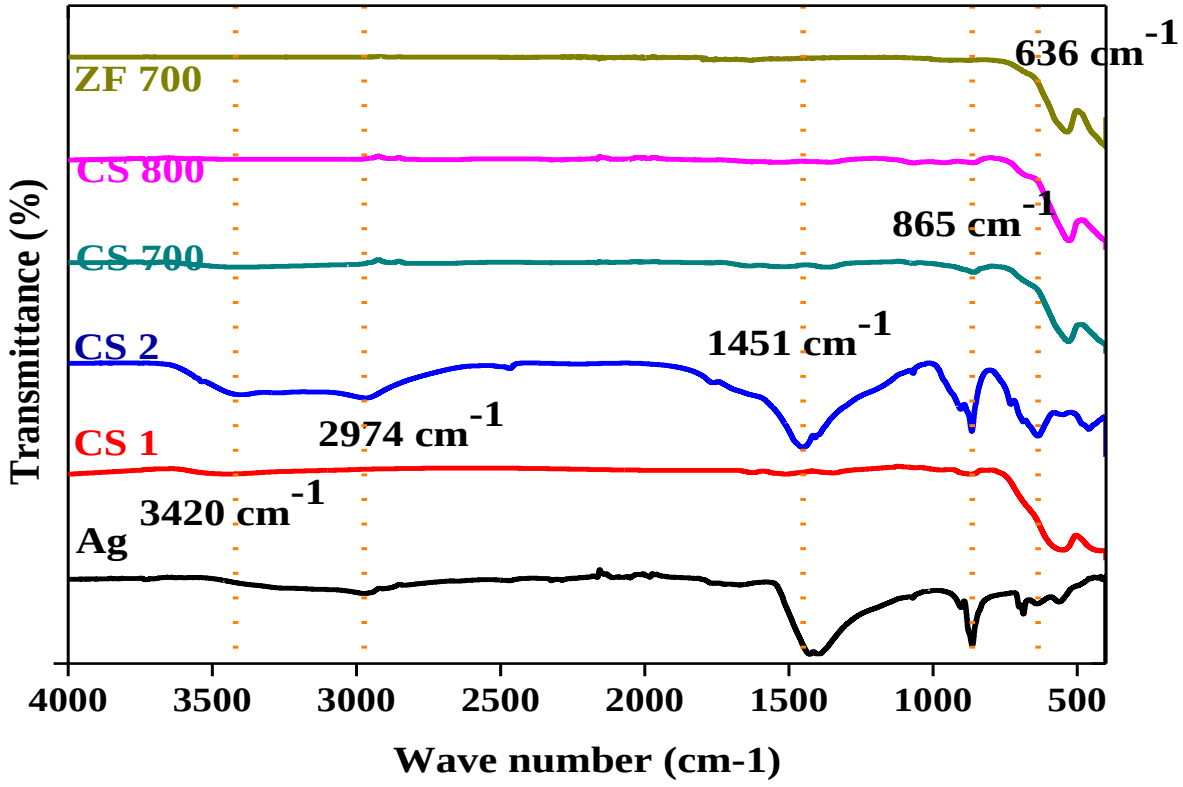

Figure 3.12 FTIR spectrum of ZF/AgCl-Ag Nanocomposite

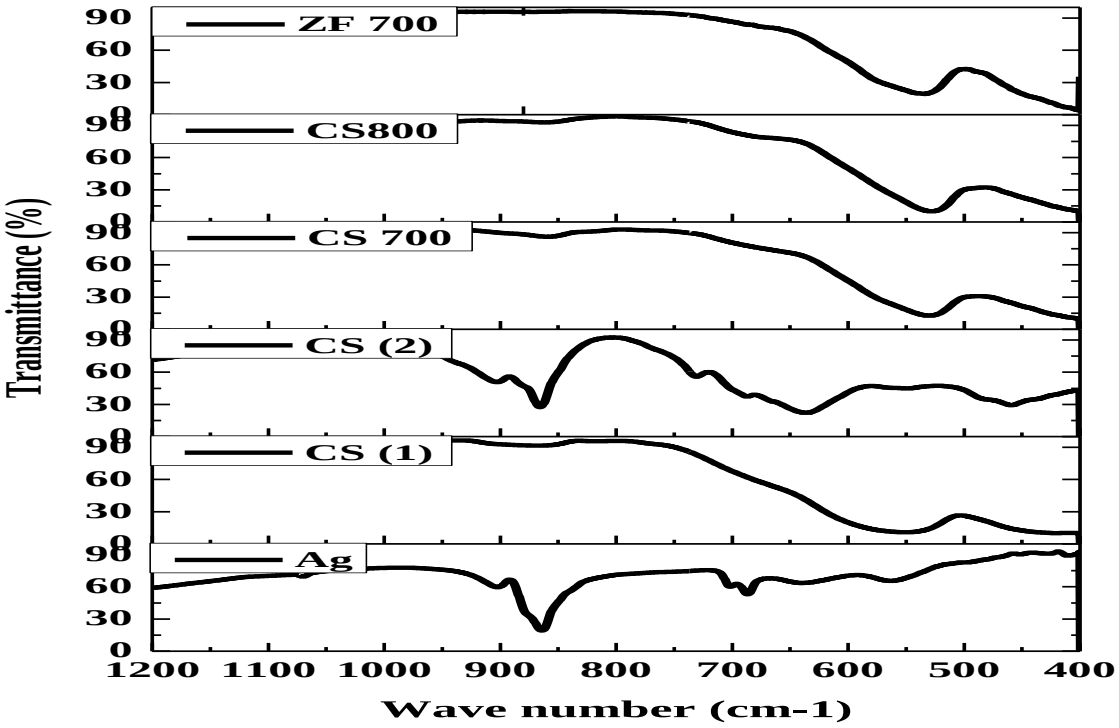

Figure3.13 FTIR spectrum showing wavelength Shift

Table 3.5 Vibrating frequency of ZF/AgCl-Ag nanocomposite.

Sl.No	Wave number (cm^{-1})	Chemical Bond
1	400.5	Fe-O vibration at octahedral site.
2	533	Zn-O Vibration at tetrahedral site
3	1451	-OH- stretching
4	636	-C=C- Stretching
5	865	-CH3- deformations
6	2974	-CH- Stretching
7	3420	-OH- Stretching

3.3.3 Vibrating Sample Magnetometer (VSM) Studies

The VSM studies reveal that all the samples are having super paramagnetic nature. Compared to the Zinc Ferrite nanoparticles the magnetization is less. But compared to the paramagnetic silver these composite samples have 10-4 times squareness ratio The absence of hysteresis suggests that the material can be easily magnetized. Thus the magnetic materials can be retrieved by applying magnetic field.

Table 3.6 Magnetic parameters of ZF/AgCl Composites

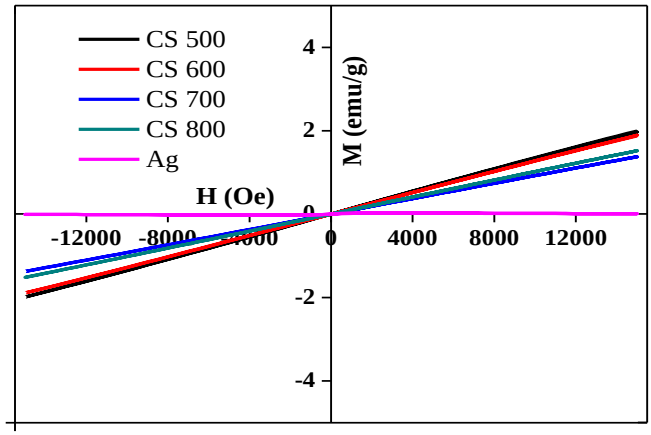

Sample	Ms (emu/g)	Mr (emu/g)	Squareness ratio (Mr/Ms)
Ag	0.023	4.51E-03	1.96E-01
CS500	1.992	3.38E-05	1.70E-05
CS600	1.891	1.50E-05	7.95E-06
CS700	1.375	1.10E-04	8.02E-05
CS800	1.518	1.84E-04	1.21E-04

Figure 3.14 M-H curve of ZF/AgCl Composites

3.4 Applications Of Zinc Ferrite Nanocomposites ($ZnFe_2O_4$/AgCl-Ag)

3.4.1 Photocatalytic Degradation Of Methylene Blue Dye

The different samples were tested for degradation of methylene blue dye (10ppm) in darkness for 15 minutes and 3 hours in sunlight. Dosage of dye was 1g/L.

The absorption spectrum of each of the samples are taken for every 30 minute interval

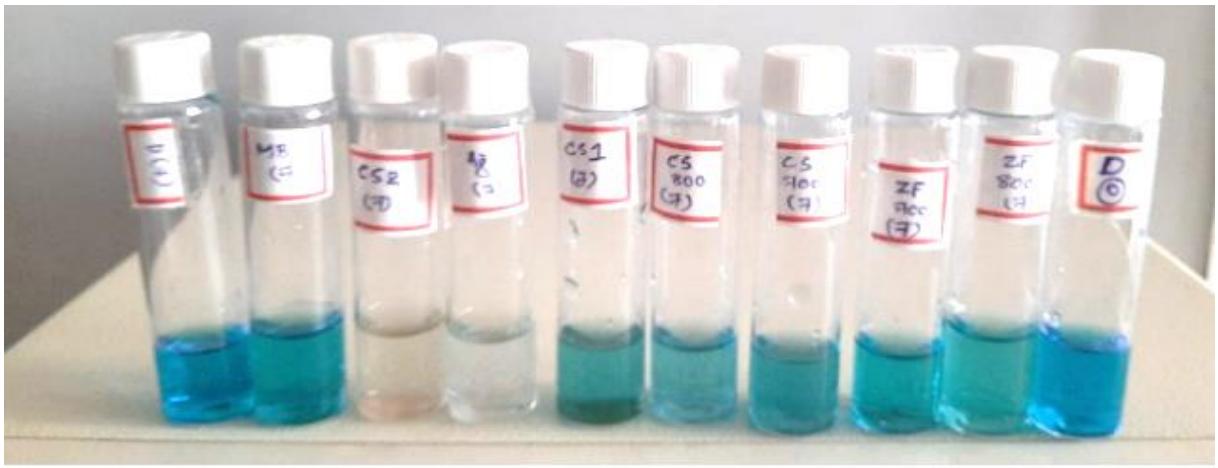

.

***Image 3.16 Photo degradation of methylene blue dye by ZF/AgCl-Ag nano composite at the seventh exposure(210 min) is compared with pure silver nanoparticles and zinc ferrite nanoparticles given in the order*ed(7), MB(7), CS2(7), Ag(7), CS1(7), CS800(7), CS700(7), ZF700(7), ZF(800), D(0)**

Absorption Spectrum of Samples at Different Intervals of Time

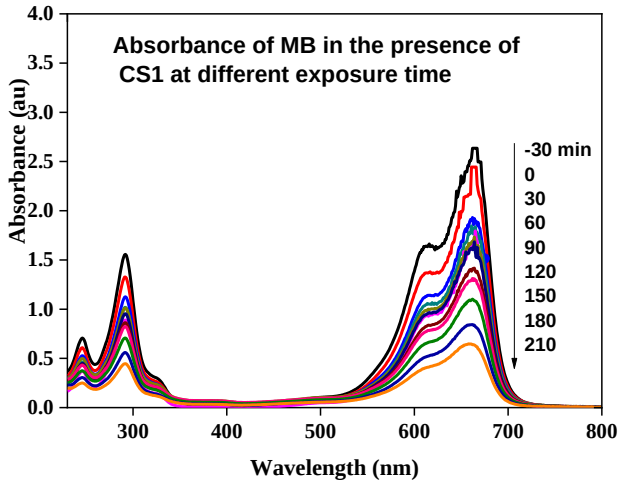

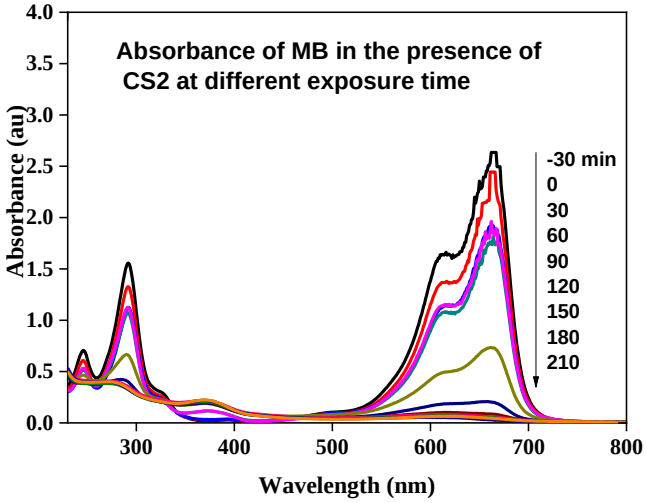

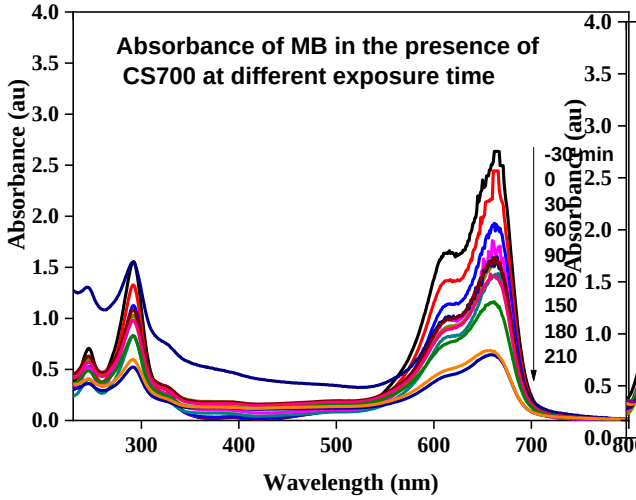

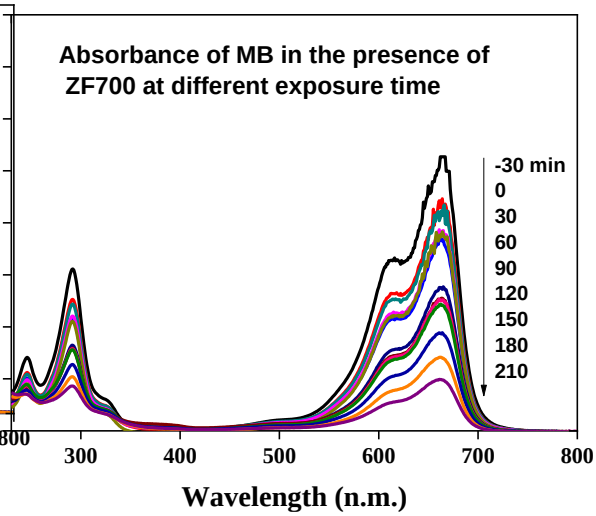

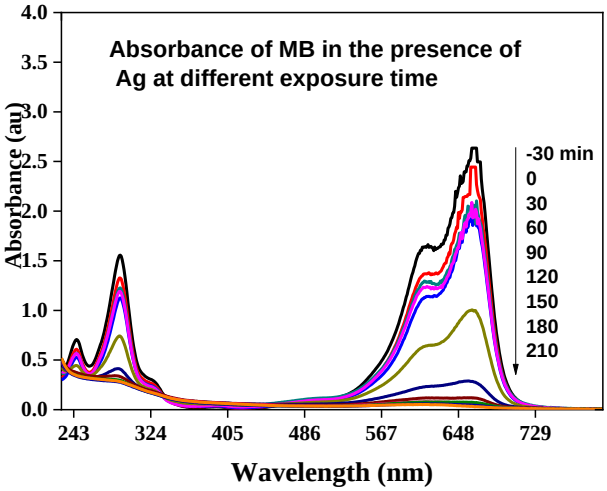

Image 3.17 Photo degradation of methylene blue dye by ZF/Ag nano composite (Sample CS2)

Absorption Spectrum of Different Samples in Same Intervals of Time

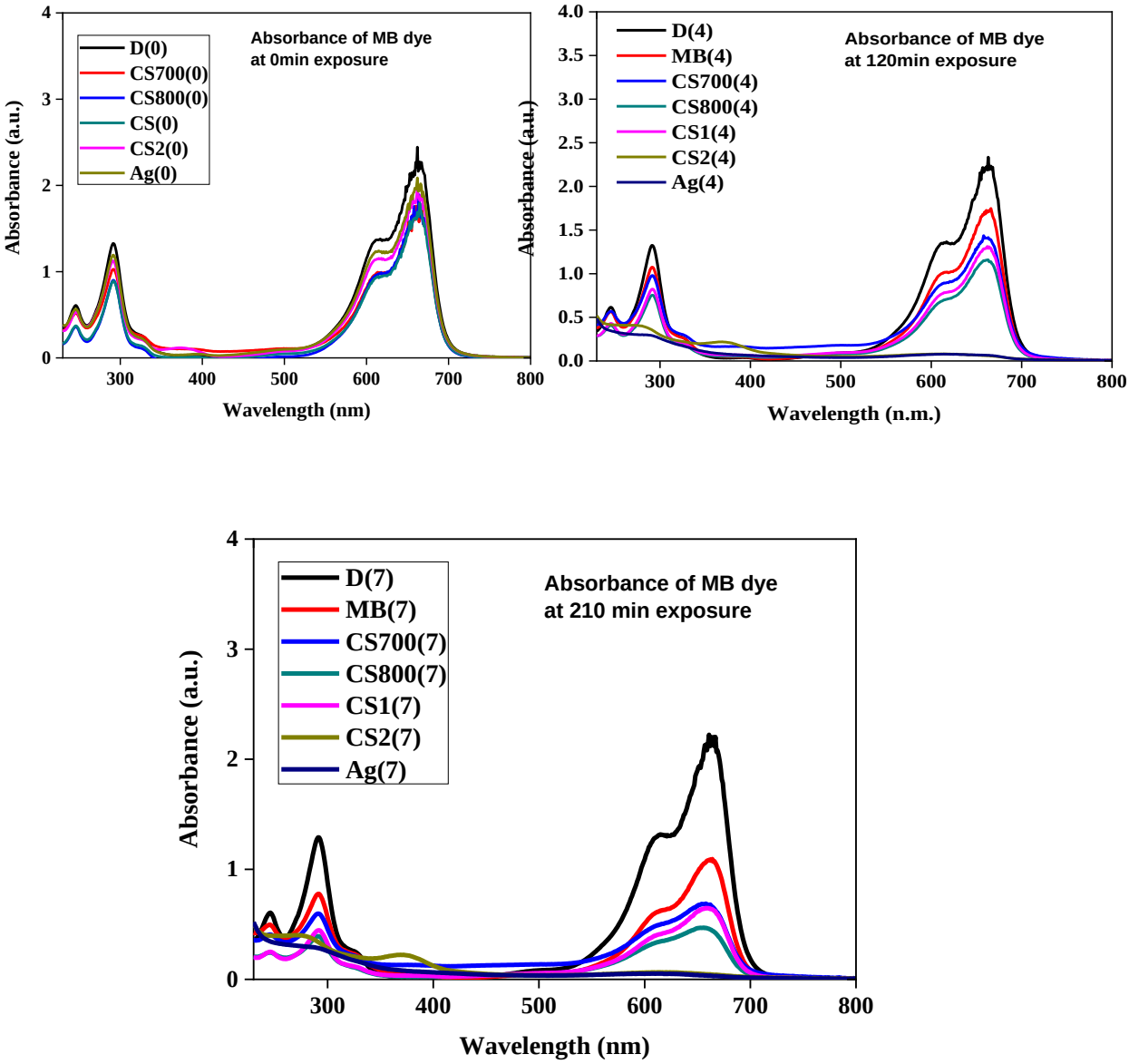

Figure 3.17Absorbance of MB dye in the presence of different photo catalyst at 0 min, 120 min and 210 min sunlight exposure

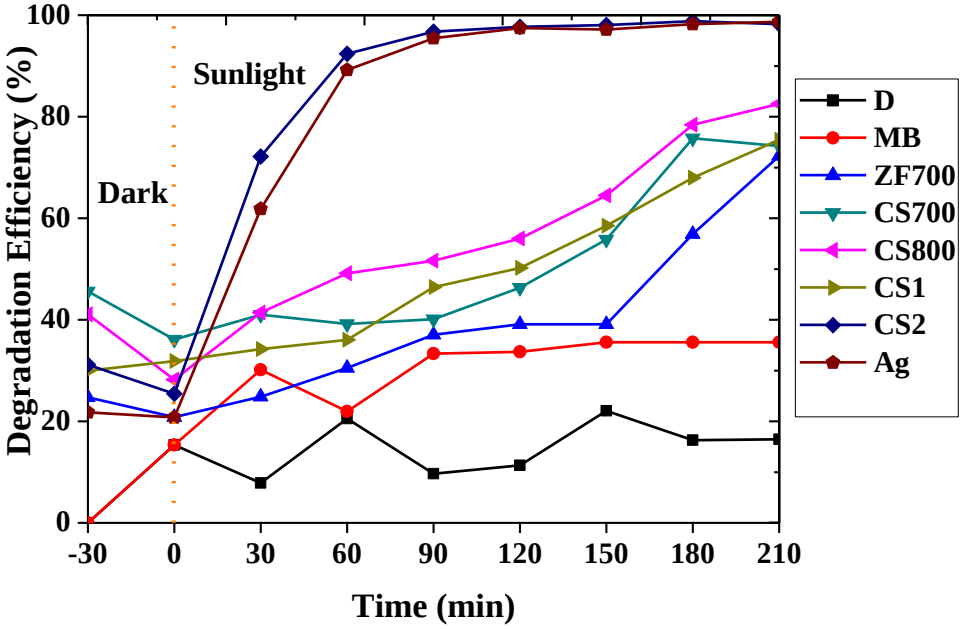

Figure 3.18 Degradation Efficiency of Zinc Ferrite Nanoparticles

The photo catalytic effects of different samples were compared. Among these CS2 and Ag have maximum degradation efficiency (98%). Therefore they are the best samples showing photo degradation of methylene blue dye in the presence of sunlight.

Table 3.7 Degradation Efficiency of Composite Nanoparticles

Sample	Degradation Efficiency (%)
CS700	75
CS800	82
CS1	76
CS2	98
Ag	97

3.4.2 Antibacterial Studies

Activity against bacteria was tested for different samples using well diffusion method. Both gram positive and gram negative bacteria are selected.

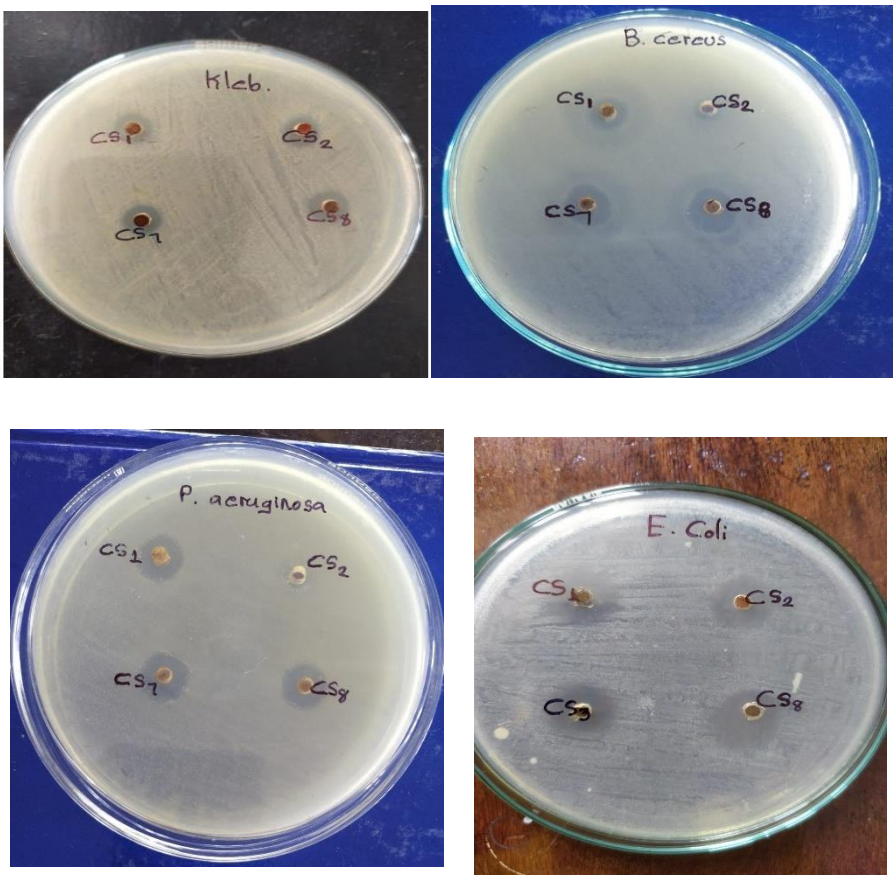

Image 3.18 Well Diffusion Method to study Antibacterial Properties

Table 3.9 The zone of inhibition against gram positive and gram negative bacteria

Samples	E.Coli	Klebscella p.	Pseudomonas	Enterococcus	Bacillus	Staph.Auereus
CS700	**13**	**7**	**12**	**10**	**12**	**9**
CS800	**14**	**7**	**11**	**10**	**13**	**8**
CS1	**13**	**10**	**12**	**10**	**11**	**9**
CS2	**11**	**7**	**-**	**6**	**6**	**4**

The composite sample shows antibacterial property. The maximum activity is shown by CS800.

CHAPTER 4

CONCLUSION

Zinc ferrite nanoparticles and its nanocomposite forms with silver and silver chloride were synthesized at different calcination temperatures using co-precipitation method. Structural characterizations confirmed the formation of cubic lattice of spinel ferrite with crystallites of zinc ferrites in the range of 15-38nm. Optical and magnetic characterization revealed the visible light active and super paramagnetic nature of the synthesized samples. Samples calcined at higher temperatures exhibited greater activity as a result of improved crystallinity. Photo degradation of methylene blue dye using the synthesized samples was analyzed. Slow degradation kinetics was observed for zinc ferrite nanoparticles with degradation efficiency of about 80% but only within 240 minutes of solar irradiation. Antibacterial analysis by well diffusion method showed no zone of inhibition for zinc ferrite nanoparticles making it inefficient for this application. Nanocomposite enhanced the properties making it suitable for applications. Rapid degradation kinetics was observed for nanocomposites with a degradation efficiency of 98% within 120 minutes of solar irradiation. Because of magnetic properties, nanocomposites can be simply recovered from reaction and reused almost without loss of catalytic activity. For nanocomposites, Zone of inhibition formation was seen both for gram negative and gram positive bacteria making it suitable for antibacterial applications. The zinc ferrite nanocomposites raise potential scope as a broad spectrum antibacterial agent against the evolution of drug-resistant bacteria, which facilitates targeted delivery and retrieval after disinfection by making use of magnetic field.

FUTURE SCOPE

The photo catalytic activity can be studied for different sample dosages, dye concentrations and different exposure intensity. We can also use arc lamps instead of direct solar irradiance and study the degradation.

The antibacterial investigations can be done using different methods like micro titer assay method, or Kirby Bauer disc diffusion method. Optical concentration which gives the density of bacterial strains can hence be found.

Applications of zinc ferrite nanocomposites in biomedical fields like magnetic hyperthermia, nanomedicine and as MRI contrast agents can be studied.

REFERENCES

- Pius, Minu, and Santhi Ani Joseph. "Dosage optimisation of magnetically retrievable zinc ferrite nanoparticles for photodegradation of methylene blue." *IOP Conference Series: Materials Science and Engineering*. Vol. 1233. No. 1. IOP Publishing, 2022
- Pius, Minu, Navya Joseph, and Kezia James. "Enhanced Antibacterial Activity of Novel Magnetic ZnFe2O4/AgCl Nanocomposites." *Materials Today: Proceedings* 9 (2019): 70-76.
- Naseri, Mahmoud Goodarz, et al. "Synthesis and characterization of zinc ferrite nanoparticles by a thermal treatment method." *Solid State Communications* 151.14-15 (2011): 1031-1035.
- Morrison, Shannon A., et al. "Magnetic and structural properties of nickel zinc ferrite nanoparticles synthesized at room temperature." *Journal of Applied Physics* 95.11 (2004): 6392-6395.
- Grasset, Fabien, et al. "Synthesis and magnetic characterization of zinc ferrite nanoparticles with different environments: powder, colloidal solution, and zinc ferrite− silica core− shell nanoparticles." *Langmuir* 18.21 (2002): 8209-8216.
- Aisida, Samson O., Ishaq Ahmad, and Fabian I. Ezema. "Effect of calcination on the microstructural and magnetic properties of PVA, PVP and PEG assisted zinc ferrite nanoparticles." *Physica B: Condensed Matter* 579 (2020): 411907.
- Yadav, G.K.Sivasankara & Satya, T & Pendyala, Sivakumar. (2021). Effect Of Calcination Temperature On Structural And Dielectric Properties Of Zn Ferrite Nanoparticles. Solid State Technology.
- Ladole, Chandrashekhar A. "Preparation and characterization of spinel zinc ferrite ZnFe2O4." *Int J Chem Sci* 10.3 (2012): 1230-4.

- Mozaffari, M., and H. Masoudi. "Zinc ferrite nanoparticles: new preparation method and magnetic properties." *Journal of Superconductivity and Novel Magnetism* 27.11 (2014): 2563-2567.
- Shahraki, R. Raeisi, et al. "Structural characterization and magnetic properties of superparamagnetic zinc ferrite nanoparticles synthesized by the coprecipitation method." *Journal of Magnetism and Magnetic Materials* 324.22 (2012): 3762-3765.
- Parvathi, K., and M. T. Ramesan. "Natural rubber composites filled with zinc ferrite nanoparticles: focus on structural, morphological, curing, thermal and mechanical properties." *Research on Chemical Intermediates* 48.1 (2022): 129-144.
- Tatarchuk, Tetiana, et al. "Eco-friendly synthesis of cobalt-zinc ferrites using quince extract for adsorption and catalytic applications: An approach towards environmental remediation." *Chemosphere* 294 (2022): 133565.
- Ghasemi, Amirmohammad Khosravi, et al. "Controllable synthesis of zinc ferrite nanostructure with tunable morphology on polyaniline nanocomposite for supercapacitor application." *Journal of Energy Storage* 51 (2022): 104579
- Cho, Jae-Hyeon, et al. "Modulation of magnetoelectric coupling through systematically engineered spin canting in nickel–zinc ferrite." *Journal of the American Ceramic Society* 105.4 (2022): 2655-2662.
- Thakur, Preeti, et al. "Recent advances on synthesis, characterization and high frequency applications of Ni-Zn ferrite nanoparticles." *Journal of Magnetism and Magnetic Materials* 530 (2021): 167925.